

Controlling polyurethane foam flammability and mechanical behaviour by tailoring the composition of clay-based multilayer nanocoatings†

Cite this: DOI: 10.1039/c3ta11936j

Yu-Chin Li, Yeon Seok Kim, John Shields and Rick Davis*

This study is a thorough evaluation of clay-based Layer-by-Layer (LbL) coatings intended to reduce the flammability of polymeric materials. Through a systematic variation of a baseline coating recipe, an ideal combination of the coating attributes that provides a rapidly developing coating with an optimum balance of flammability, mechanical, and physical attributes on a complex 3D porous substrate, polyurethane foam (PUF) was identified. Using a unique trilayer (TL) assembly approach, the coating growth was significantly accelerated by the polymer (poly(acrylic acid) (PAA)/branched polyethylenimine (BPEI)) concentration in the formulation. However, to significantly reduce flammability without compromising other performance attributes, the concentration of the nanoparticle fire retardant (nanoFR, clay) suspension was critical. This study has resulted in the most significant reduction in PUF flammability using LbL technology without compromising any of the mechanical or physical attributes of the PUF. More specifically, a reduction in the peak heat release rate (pHRR) and average heat release rate (aHRR) of 33% and 78%, respectively, has been achieved. This reduction in flammability is at least two times more effective than commercial fire retardants and other LbL FR coatings for PUF. The insights gained through this research are expected to accelerate the development of other LbL coatings regardless of the intended application.

Received 16th May 2013

Accepted 14th August 2013

DOI: 10.1039/c3ta11936j

www.rsc.org/MaterialsA

Introduction

Layer-by-layer assembly (LbL) is a robust and dynamic approach to fabricate multilayer thin films.^{1–3} The films are produced by repeatedly depositing alternating pairs of monolayers (called bilayers, BL). The monolayers are held together by electrostatic attraction, hydrogen bonding,^{4,5} covalent bonding,^{6,7} metal–ligand coordination complexes,⁸ and many other host–guest pairs.⁹ This fabrication process uses aqueous solutions or organic solvents, with polyelectrolytes, charged inorganic nano-substances, or biomaterials as the building blocks.¹⁰ Using an appropriate surface treatment, thin films can be deposited on a wide variety of substrates¹¹ and imbue a broad range of functionalities (*e.g.*, hydrophobic surfaces^{12,13}) for many applications (*e.g.*, electrochromic thin films,^{14,15} drug delivery,^{16,17} tissue engineering,^{18,19} and biosensing^{20,21}). There is an increasing number of commercial products based on this LbL technology.²²

Recently, LbL has been studied as a novel flame retardant (FR) platform technology for cotton fabrics,^{23–25} polyester

fabrics,^{26,27} polylactide films,²⁸ and flexible polyurethane foam.^{29–31} These LbL FR coatings are typically constructed of an inorganic nanoparticle (*e.g.*, montmorillonite (MMT), POSS, and silica) and polymers (*e.g.*, polyacrylamide). On 2-dimensional substrates (fabrics and films), these LbL FR coatings have resulted in reduced flame spread and flame extinguishment. There is very little reported and understood on using LbL to coat complex 3-dimensional substrates (foam). On foam, it appears that heat release rate is the most significant flammability characteristic that is improved with the LbL FR coatings. LbL can also suppress flame spread to the surroundings by preventing the formation of a flaming liquid material.³²

Polyurethane foam is used extensively as the comfort component in consumer and commercial furniture, mattresses, buildings, and transportation. Polyurethane foam can be a significant fire threat and often the reason a small fire rapidly transitions into a significant fire threat. Therefore, to comply with flammability regulations, the polyurethane foam is filled with FR and/or protected with a fire blocking technology. The current FR technologies are under increased scrutiny for environmental, health, and safety concerns and, alone, they are typically insufficient to enable compliance with current or proposed flammability regulations.³³ LbL may be an alternative to the current FR that enables compliance with flammability, environment, and health requirements without the need for a fire blocking technology.

National Institute of Standards and Technology, Engineering Laboratory, 100 Bureau Dr., MS-8655, Gaithersburg, MD 20899-8655, USA. E-mail: rick.davis@gist.gov; Tel: +1 301 975 5901

† Electronic supplementary information (ESI) available. See DOI: 10.1039/c3ta11936j

Kim *et al.*²⁹ first used carbon nanofibers (CNFs) as the main component of a LbL FR coating on polyurethane foam. This BL coating was constructed of an anionic layer (poly(acrylic acid), PAA) and a cationic layer created by a solution blend of CNFs and branched polyethylenimine (BPEI). This 4 BL PAA/CNF–PEI coating was 360 nm thick, contained 50% CNF, and only increased the substrate mass by 3.2%. Yet, it caused a 40% reduction in the cone calorimeter peak heat release rate (pHRR) value (a critical flammability metric), which is comparable to what commercial FRs achieve, but at a two to three times lower loading level. However, the coating also caused a 50% increase in the first HRR peak. This suggests that while the CNF LbL coating can reduce the total fire threat of polyurethane foam, the higher early-on HRR values may reduce the time to escape or defend such a fire. Additionally, the black color caused by the CNF may be an aesthetic deterrent to commercialization.

Kim *et al.*³¹ failed to produce a MMT LbL coating on polyurethane foam using the traditional BL approach (BPEI cationic/MMT anionic). At 20 BLs, there was less than 1% mass gain with only 100 nm thick coating. The researchers then used a novel approach of inserting another anionic layer (PAA) between the BPEI and MMT layers (BPEI/MMT/PAA). This tri-layer (TL) approach resulted in exponential film growth and a high MMT content. At 8 TLs, the coating was 1000 nm thick, contained 64% MMT, and increased the polyurethane foam mass by 3.2%. A 17% reduction in pHRR was reported with this coating. Compared to the CNF BL system, the MMT coating was thicker, contained a higher inorganic content, and was less effective at reducing polyurethane foam flammability. Both coatings had two HRR peaks and caused an approximate 50% increase in the HRR value of the first peak.

After two significant changes to the recipe, Davis *et al.*³⁴ developed a MWCNT LbL coating on polyurethane foam that exhibited a similar FR performance as the previously reported CNFs. The first significant change was to covalently attach BPEI to the surface of the MWCNT to facilitate dispersion and adhesion in the coating. The second change was to use the TL approach to further increase MWCNT retention and promote faster film growth. The 4 TL BPEI/MWCNT–BPEI/PAA coating was 440 nm thick, contained 51% MWCNTs, and increased polyurethane foam mass by 3.4%. The reduction in the pHRR value was 35% for this coating. Similar to both the MMT TL and CNF BL coatings, the MWCNT TL coating also had two HRR peaks and caused an approximate 50% increase in the HRR value of the first peak.

Laufer *et al.*³⁰ recently used an all-natural ingredient (chitosan and MMT) as the building block for a LbL FR coating on polyurethane foam. This 4 mass% and 10 BL coating caused a 50% reduction in the pHRR value. Similar to the previously mentioned coatings, this chitosan–MMT coating also had two HRR peaks in the cone. However, for the first time the HRR value for the first peak was lower than that measured for the uncoated polyurethane foam. This coating is promising, but it is unclear whether the performance can be directly compared to the coatings reported by Davis and Kim^{29,31,34} as the polyurethane foam used by Laufer was polyester based polyurethane (typically used for filtering and not furniture) and the flammability test specimens were only 2.5 cm thick, rather than 5.0 cm.

The most effective LbL FR coating on non-fire retardant ether-based flexible polyurethane foam (PUF) to date is reported here. This study is a comprehensive evaluation of the impact of variations of a clay-based LbL coating formulation on PUF on the fire performance, mechanical and physical properties of the applied foam. The impact of a systematic change of the recipe on the film growth rate on PUF, and on the PUF's mechanical performance and flammability is discussed. This research reveals an ideal combination of coating attributes in the composition that, in the least number of layers, provides the best combination of flame reduction while still maintaining critical PUF mechanical attributes.

Experimental^{35,36}

Unless indicated all materials were used as received.

Chemicals and substrates

Branched polyethylenimine (BPEI, $M_w \sim 25\,000$) and poly(acrylic acid) (PAA, $M_w \sim 100\,000$, 35 wt% in H_2O) were purchased from Sigma-Aldrich (Milwaukee, WI). Sodium montmorillonite clay (MMT, trade name Cloisite Na⁺) was obtained from Southern Clay Products Inc. (Gonzales, TX). Water purified in a Nanopure II system (18.2 M Ω cm, Sybron/Barnstead) was used for all wash and depositing solutions. Standard polyurethane foam (not flame retarded, 29.1 kg m⁻³ density) received from FXI Inc. (Media, PA) was stored in black plastic bags in a conditioning room (25% relative humidity and 23 °C \pm 2 °C) until it was cut for coating ((10.2 \times 10.2 \times 5.1) \pm 0.1 cm³). This PUF was used for cone and compression testing. The PUF was cut in half (2.50 cm thickness) for airflow testing. Prior to coating the PUF was dried in a desiccator for two days. Immediately before coating, the mass of the dry PUF was measured and was used to calculate the mass gained from the coatings.

Layer-by-layer deposition

A schematic process of LbL is shown in Fig. 1. Polymer solutions and MMT suspensions used for coating fabrication were both prepared at a low and a high concentration. Polymer solutions were 0.1% and 0.5% polymer by mass. The MMT suspensions were 0.2% and 1% MMT by mass. Four different concentration combinations were created: LL, LH, HL and HH, as seen in Fig. 1b. The first letter stands for the concentration of polymers and the second one stands for clay concentration. Before coating, the PUF was pre-soaked in a 0.1 N HNO₃ solution for 5 min in order to create a positively charged surface on the PUF. Excess acidic solution was squeezed out, then the PUF was soaked in the first negatively charged polyelectrolyte solution (PAA, 700 mL) for 5 min. Excess PAA was squeezed out and then the PUF was washed in DI water. Excess water was squeezed. This completes the deposition of the first PAA monolayer. This same series of activities were repeated next using a positively charged solution to deposit the first BPEI monolayer on the PAA monolayer. These steps were repeated again using a MMT suspension to place the MMT monolayer onto the PAA/BPEI

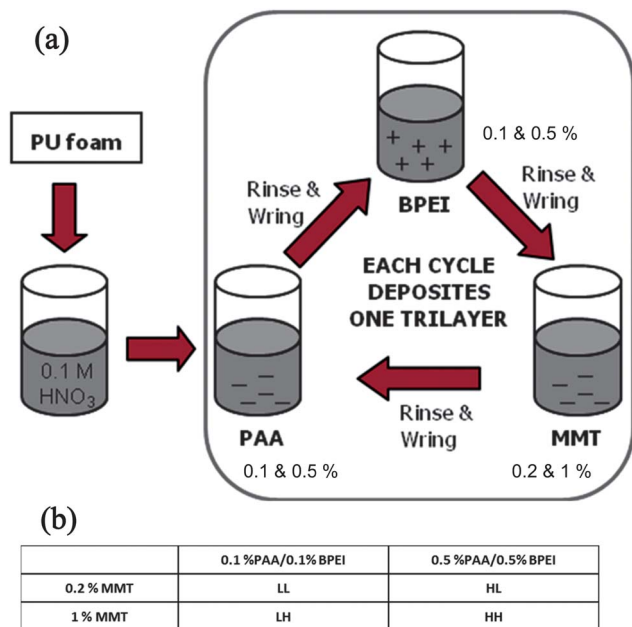


Fig. 1 (a) Schematic of the LbL deposition process on PU foam. Foam was first dipped in an acidic solution and placed in coating solutions without rinsing. The foam was coated with PAA, BPEI and then MMT, until the desired number of layers was reached. Between each deposition the foam was rinsed with DI water. The concentrations of the dipping solutions are listed, and the concentrations of the solutions for four different systems: LL, LH, HL, and HH are listed in (b).

bilayer. This completes the fabrication of the first trilayer. This same series of steps were repeated until the desired number (3, 5, and 7) of trilayers is deposited with the exception that the soak time was reduced to 1 min. Water was removed from the coated foam by placing in a $70\text{ }^{\circ}\text{C} \pm 3\text{ }^{\circ}\text{C}$ convection oven overnight and then storing in a desiccator for one day. The coating mass was calculated from the mass measured before and after coating using a laboratory microbalance. The average mass of each recipe was obtained from 4 coated samples.

Thermogravimetric analysis

The mass of MMT was measured with a TG 449 F1 Jupiter® Thermogravimetric analyzer (TGA, Netzsch, Burlington, MA). In breathing quality air, a 10 mg specimen was heated up to $90\text{ }^{\circ}\text{C}$ and isothermed for 30 min, then the temperature was increased from $90\text{ }^{\circ}\text{C}$ to $850\text{ }^{\circ}\text{C}$ at a heating rate of $20\text{ }^{\circ}\text{C min}^{-1}$. The MMT content on PUF was the residue mass measured using TGA. The MMT content in the coating was calculated using the TGA residue and the mass of the coating was measured using a microbalance.

Cone calorimetry testing

A dual cone calorimeter operating at 35 kW m^{-2} with an exhaust flow of 24 L s^{-1} was used to measure the flammability of the control and coated PUF. The experiments were conducted according to standard testing procedures (ASTM E1354-07). A cone size sample ($(10.2 \times 10.2 \times 5.1) \pm 0.1\text{ cm}^3$) was placed in a pan constructed from heavy gauge aluminum foil. The sides

and bottom of the sample were covered by the aluminum foil such that only the top surface was exposed to the cone heater. The standard uncertainty is $\pm 5\%$ in HRR and $\pm 2\text{ s}$ in time.

Scanning electron microscopy

A Zeiss Ultra 60 Field Emission-Scanning Electron Microscope (FE-SEM, Carl Zeiss Inc., Thornwood, NY) was used to acquire surface and freeze-fractured specimens of the coatings on the PUF. All SEM samples were sputter coated with 8 nm of Au/Pd (60%/40% by mass) prior to SEM imaging.

Compression test and airflow of PUF

PUF modulus and airflow as a function of the number of TLs were measured according to industry standards, which is the first time these critical PUF attributes have been reported for any LbL coated PUF. Compression tests were performed using a Universal Testing Machine (Instron 5500R, Instron Corp., Canton, MA). This test was conducted according to ASTM D3574, except that the PUF size and thickness do not fulfill the requirement of the standard method, and a smaller diameter indenter foot was used. Therefore, the test results are intended to provide a relative comparison and not absolute values to compare against commercial specifications. The flat circular indenter (25 mm in diameter) was brought in contact with the surface of the PUF without contact force. The PUF was indented 65% of the foam thickness at a cross-head at 5 mm min^{-1} and then held in that position for 3 s. The indenter was then retracted. The force measured to compress the PUF and applied by the PUF during retraction was measured and plotted as a function of % indentation of the foam.

An electronic high differential pressure air permeability-measuring instrument (FAP 5352 F2, Frazier Precision Instrument Co. Inc., Hagerstown, MD) was used to measure air permeability for control and coated PUF. The $1.3\text{ cm} \pm 0.1\text{ cm}$ PUF was placed in a circular clamp, exposing 38.5 cm^2 of the foam to a perpendicular airflow. The target pressure-drop through the 1.3 cm thick PUF slice was set to 127 Pa (13 mm of water). A nozzle with an orifice diameter of 11.0 mm was used to reach the target pressure drop. The permeability (Φ) in terms of volumetric air flow was read in cubic feet of air per square foot of sample area per minute (CFM) at $20\text{ }^{\circ}\text{C}$ and 1 atm.

Results and discussion

A MMT-based TL coating evaluated on foam typically used in residential furniture in the United States was studied; *i.e.*, polyether polyol and toluene diisocyanate polyurethane foam (Formulation A8 from CPSC report³⁷) and air permeability of $284.75\text{ ft}^3\text{ min}^{-1}$. The components of this TL coating are PAA/BPEI/MMT. Two different mass concentration polymer solutions (BPEI and PAA at 0.1% (low) and 0.5% (high)) are paired with two different mass concentration MMT suspensions (0.2% (low) and 1% (high)). Four different concentration combinations were created (polymer/MMT): low/low (LL), low/high (LH), high/low (HL), and high/high (HH).

Layer-by-layer process and coating growth on PUF

LbL BL films constructed of PAA and PEI have been extensively studied.^{38–40} The processing/fabricating conditions (*e.g.*, pH) significantly influence the coating thickness of this pure polymer coating with the thickest coatings achieved with as-dissolved pH values (10.5 for BPEI and 3.2 for PAA).³⁸ Under most conditions the growth rate is exponential. LbL BL films of BPEI and MMT have more recently been studied for gas barrier and flammability reduction applications.^{23,41,42} Compared to the pure polymer system, this polymer and MMT coating grows at a much slower and linear rate with the thickness controlled by the pH value of the BPEI solution^{23,41} and the concentration of the MMT suspension.²³ The novel TL approach (BPEI/MMT/PAA) introduced by Kim *et al.*³¹ appears to be a cross of these two BL systems with an exponential coating growth (similar to pure polymer, but significantly slower) and a high concentration of MMT in the coating (60 mass%). In these studies, the films were grown on a silicon wafer (Ellipsometry) and quartz crystal (Quartz Crystal Microbalance). In the TL study, the thickness of 8 TL coating was measured on the PUF using SEM. The thickness value measured on PUF was significantly thicker suggesting that the QCM and Ellipsometry were best used to understand coating trends and not to accurately measure the coating thickness on PUF.

The mass of the coatings of PUF as a function of the number of TLs for the LL, LH, HL, and HH compositions is provided in Fig. 2. The first step to rapid film growth was to strengthen the interaction between the polymer and PUF, which was achieved by soaking PUF in 0.1 M nitric acid solution prior to coating.

For 1 TL, the mass of the coating was independent of depositing solution concentration ($0.9\% \pm 0.2\%$ by mass). At 3 TLs, the mass of the coatings diverged based on the polymer concentration. The high polymer concentration formulations (HH and HL) resulted in a coating mass of $8.0\% \pm 0.3\%$, whereas the low polymer concentration formulations resulted in 37% lighter coating ($5.0\% \pm 0.3\%$ by mass). With the higher number of TLs, this trend continued, but the difference in the

coating mass became increasingly more significant. At 5 TLs, the high polymer formulations were 70% heavier than the low polymer formulations ($25.0\% \pm 2.5\%$ by mass as compared to $7.5\% \pm 0.3\%$ by mass). At 7 TLs, the coating mass appeared to plateau/slow down. The high polymer formulations were 75% heavier than the low polymer formulations ($31.0\% \pm 0.1\%$ by mass as compared to $8\% \pm 0.3\%$ by mass). These data indicate that the coating mass growth is controlled by the concentration of the polymer depositing solution and the MMT concentration has a minimal impact. The 3 TL systems appear to be the most interesting ones, as the coating mass is not that significantly different between these four formulations, which may allow us to further understand how the coating composition, *i.e.*, MMT to polymer ratio, impacts flammability and physical attributes.

Scanning electron microscopy was used to visually characterize the PUF and LbL coatings. Select images of LH and HH formulations are provided as representative images. The natural porous structure and smooth surface feature of the PUF can be seen in Fig. 3a and b. With 1 TL of LH, the surface appears rough even at low magnification. The MMT is well distributed across the entire PUF surface with occasionally larger aggregates observed (Fig. 3c and d). Both of these observations are understandable given that the coating at this point is 80% by mass of MMT. Though the MMT content in the coating decreases by approximately a factor of 2 to 3 with a higher number of TL (due to the interdiffusion of polymers), the total MMT content increases by a factor of 2 to 7. The result is that with more TLs the coating surface becomes increasingly rougher; *e.g.*, LH3 (Fig. 3e and f), and HH7 (Fig. 3g and h).

The coating thickness of a cross-sectional freeze fracture substrate was measured using a SEM. The thickness values trended with the coating mass. One of the best FR formulations, LH3 (discussed later), had a coating thickness of $344 \text{ nm} \pm 20 \text{ nm}$.

The coating mass of the 8 TL BPEI/MMT/PAA of PUF is plotted as ● in Fig. 2 (Kim *et al.*³¹). Using the nitric acid presoak, we achieved a similar coating mass using six less TLs (only 2 TLs). This equates to depositing 24 less monolayers. This indicates that the nitric acid presoak is critical for fast coating growth and enables a larger dynamic range of coating masses. At 0.1 M, there is minimal oxidation of the polymer and 93% dissociation of the acid.⁴³ Therefore, it is assumed that an increased charged density on the PUF, created by the dissociated nitric acid ions interacting with the polar functionality and protonation of the polyurethane polymer, promoted adhesion of the PAA anionic first layer.

Since the same depositing solutions were used for each TL, the concentration of polymer and MMT in the depositing solutions decreased as the number of TLs increased. To determine if the plateau of mass coating growth at a higher number of TLs was a result of decreased solution concentration or a limit of the coating process, all depositing solutions for LH were replaced at 4 TLs with freshly prepared LH solutions. The result was a 50% increase in the coating mass at 7 TLs (13.5% as compared to $7.5\% \pm 0.1\%$ by mass). This observation suggests that another parameter to increase coating growth is to use depositing solutions where the concentration is sufficient to not

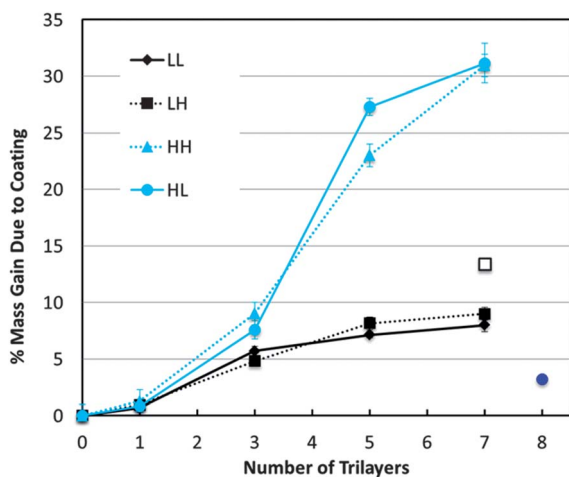


Fig. 2 Mass growth of LL, LH, HH and HL systems of PU foam as a function of TL numbers. 8 TLs from a previous study (●),³¹ and LH 7 with the dipping solutions refreshed at 4 TLs (□) are also shown for comparison.

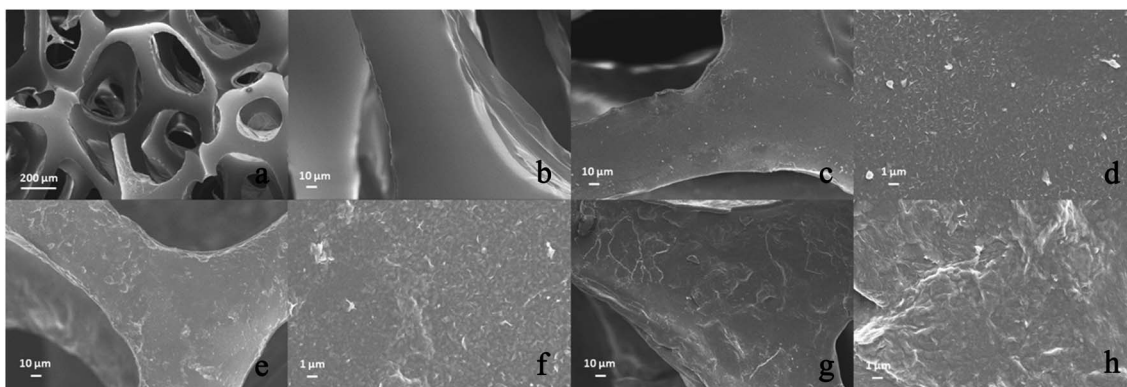


Fig. 3 SEM images of control foam (a and b), LH1 (c and d), LH3 (e and f), and HH7 (g and h) coated foams.

be a limiting factor; *e.g.*, using continuously circulating baths with real-time monitoring. This also further illustrates that the highest coating mass in the least number of layers is only possible using high (H) polymer formulations.

Until the TL approach was introduced, LbL coatings were fabricated by alternately depositing oppositely charged monolayers and it is this charge, which can be very weak, that allows these monolayers to adhere to each other and grow a coating. From this conventional LbL point of view, this TL approach should not work as the MMT and PAA are both anionic monolayers. The data presented in Fig. 2 not only show that a TL coating can grow, but with an appropriate surface treatment the coating can grow faster and significantly increase the mass uptake. The rapid coating growth of PAA and BPEI is well documented and is attributed to interdiffusion of the depositing polymer onto the existing polymer coating, which causes an increase in the surface charge density that promotes thick polymer deposition.^{38,39} Presumably the attraction between MMT and PAA is hydrogen-bonding between edge and surface hydroxyls on MMT with the acrylic acid groups of PAA.⁴⁴ This attraction appears to overcome the anionic repulsive forces.

Cone calorimetry and thermal analysis of coated PU foam

Cone calorimetry is a standard approach to test material flammability under a constant external heat flux (35 kW m^{-2}) (ASTM E-1354). This test simulates a developing fire scenario. Values measured are routinely used to define the flammability of a material and this is the basis of many performance flammability standards and regulations. The most common parameters of interest are time to ignition (TTI), the maximum peak heat release rate (pHRR) for the HRR curve, the time to pHRR (t-pHRR), the total heat released (THR), and the average HRR (aHRR) value during the test. Cone data are typically plotted as the HRR as a function of time in the test.

The cone curves are plotted as a function of solution concentration in Fig. 4 (LL (a), HL (b), LH (c), and HH (d)). Each graph is a stack plot of HRR curves of the control PUF and the coated PUF as a function of the number of TLs. The values of important parameters measured in the cone are provided in Table 1.

The PUF HRR curve consists of two peaks associated with the combustion of polyisocyanate (first and smaller HRR peak) and polyol (second and larger HRR peak). The HRR values for these peaks are $377 \text{ kW m}^{-2} \pm 17 \text{ kW m}^{-2}$ and $451 \text{ kW m}^{-2} \pm 23 \text{ kW m}^{-2}$, respectively. All the 1 TL coatings still have two peaks, but the second peak has been reduced by 28% (HH1 and LL1) to 44% (LH1). In all cases, the first peak has now the highest HRR value for the curve (pHRR), which is the reason why the t-pHRR has decreased from the $86 \text{ s} \pm 4 \text{ s}$ for PUF to 23 s to 41 s for the 1 TL coatings. The reduced time to peak is not a concern because even with 1 TL, the PUF flammability has been greatly reduced: the pHRR value has been reduced by 14% (HL1) to 24% (HH1) and the aHRR has been reduced by 33% (HL1) to 50% (LH1).

At higher numbers of TL, all formulations further suppress the second peak and reduce the aHRR value. However, the magnitude is strongly dependent on the number of TL and the coating composition. The LL formulation (Fig. 4a) shows a fairly consistent reduction and delaying of the second peak with an increasing number of TL. The aHRR and pHRR values have decreased by at most 63% and 26% (LL7), respectively.

Increasing the polymer concentration (HL, Fig. 4b) reduces the number of layers needed to reduce aHRR and HRR of the second peak, and improves the maximum FR impact of the coating. At 3 TLs, HL already delivers a reduction in aHRR and HRR of the second peak that is comparable to the best LL formulation (7 LL). The higher number of TL only slightly reduces the aHRR and HRR of the second peak. The best reduction in aHRR and pHRR is 63% (HL5 and HL7) and 29% (HL5), respectively. The dramatic difference, which will be discussed below, is how quickly the HRR value drops off after the first peak and the plateau value at the end of the rapid drop off.

Increasing the MMT rather than the polymer concentration has a more dramatic impact on flammability (LH, Fig. 4c). At 3 TLs, 5 TLs, and 7 TLs for LH, the second HRR peak is completely gone. This is the first report of the second peak in LbL PUF ever being completely suppressed. There is no discernible difference in the HRR curves at and above 3 TLs, suggesting that a plateau in the flammability reduction has been reached with this formulation. The largest reduction in aHRR and pHRR was 73% and 30% (LH5 and LH7), respectively.

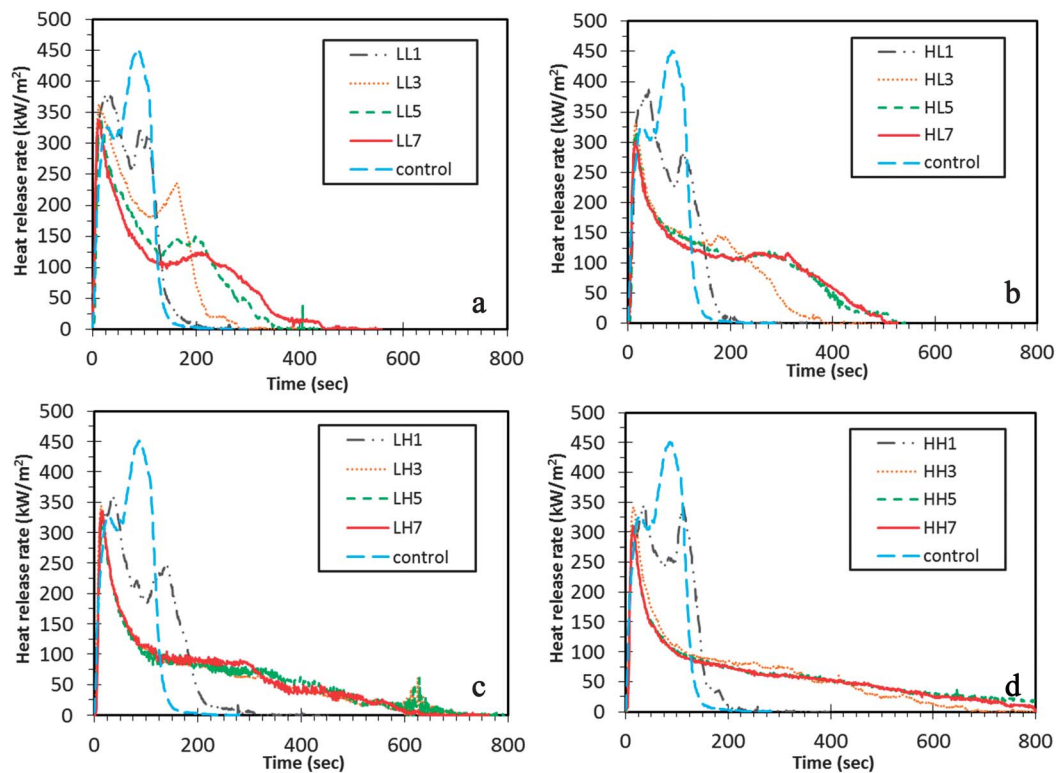


Fig. 4 Heat release rate curves of control and 1, 3, 5, and 7 TLs of LL (a), HL (b), LH (c) and HH (d) systems of coated foams.

Table 1 Cone calorimetry data of uncoated and MMT-coated samples. Except 1 TL, the rest of the coated foams showed only 1 peak and reduced PHRR, lower average HRR, and longer burning/smaller energy release over time

	Coating mass %	pHRR (kW m ⁻²)	t-PHRR (s)	aHRR (kW m ⁻²)	Residual mass %	Burn time (s)
Control	—	451	86	275	—	154
LL1	0.7	377	23	181	6.7	223
LL3	5.7	353	14	163	5.6	360
LL5	7.1	342	12	123	4.8	282
LL7	8.0	337	12	101	4.7	446
LH1	1.0	353	36	138	7.7	317
LH3	4.8	345	13	82	5.2	690
LH5	8.2	335	17	76	5.0	724
LH7	9.0	325	14	74	5.8	632
HL1	0.8	387	41	183	7.0	221
HL3	7.5	331	15	113	6.7	383
HL5	27.4	317	16	100	5.8	529
HL7	31.2	302	16	104	6.8	506
HH1	1.5	343	35	168	7.3	240
HH3	9.9	342	16	70	7.5	670
HH5	21.5	303	15	57	10.7	879
HH7	30.6	309	15	59	12.7	798

At a high MMT concentration (LH), increasing the polymer concentration (HH, Fig. 4d) yielded no significant reduction in PUF flammability. At 3 TLs or greater there is no second HRR peak. The greatest reduction in aHRR and pHRR is 78% and 33% (HH5 and HH7), respectively.

These LbL coatings are a condensed phase FR, which means that material flammability is reduced by disrupting the

pyrolysis process in the substrate. More specifically, a residue is formed on the surface of the substrate that reduces thermal conduction into the substrate and the release of pyrolysis products that are fuel for the combustion process in the gas phase. Typically, the evaluation of a condensed phase FR is based primarily on the magnitude of the pHRR reduction. However, the fire threat depends on the completeness, effectiveness, and the durability of the residue, which is more accurately quantified by the aHRR value.

The HRR curves (Fig. 4) indicate which formulations are the most effective and the photographs and SEM images helps us to understand why they are effective (Fig. 5 and 6). A narrower first peak and a more rapid drop in HRR indicates a more effective FR residue, *i.e.*, faster forming, denser, thicker, and/or less cracks. A smaller or the absence of a second peak combined with a lower HRR plateau value indicates a more durable FR residue. For the less effective formulations (LL and HL), the residue becomes thicker with less imperfections (*e.g.*, cracks, holes, and thin areas) with increasing numbers of TL, which is the reason why the first peak becomes increasingly narrower and the second peak becomes smaller. For the very effective formulations (LH and HH), there is no second peak and very low HRR plateau values above 1 TL. The above 1 TL residues are thicker and have little to no imperfections, which is why the residues are so effective at reducing and maintaining low HRR values throughout the test. In some of these formulations, the residue size is comparable to the original PUF and still retains the PUF cell structure (Fig. 6).

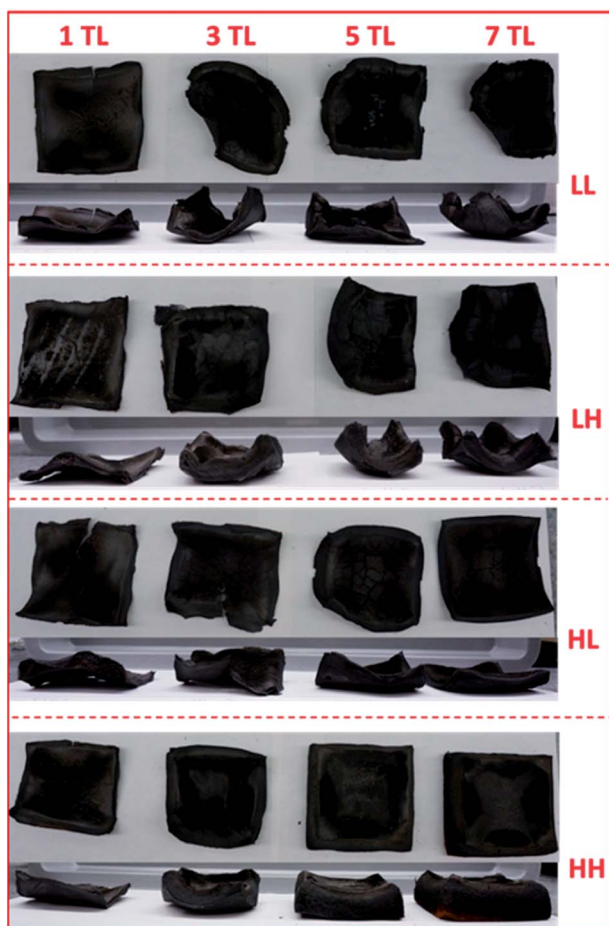


Fig. 5 The photographs of all coated foam after cone calorimetry.

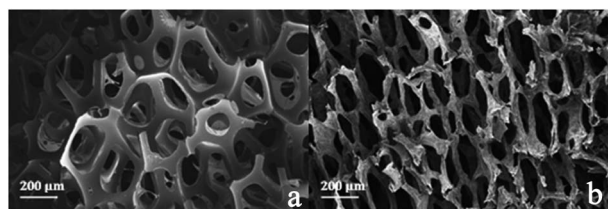


Fig. 6 Cell structure of control foam (a) and HH5 coated foam after cone calorimetry (b) under SEM imaging.

The coatings previously reported for PUF have HRR curves, which contain two peaks.^{29–31,34} The aHRR values were not reported for the CNF,²⁹ MWCNT,³⁴ and the MMT³¹ coatings. However, a qualitative comparison of those HRR curves with the HRR curves reported here suggests that those coatings are no better than the LL1 or HH1 formulations reported here. Compared to our best formulations (LH3 or HH3 MMT coatings), the 10BL chitosan–MMT³⁰ coating is 12% better at reducing pHRR, but 40% less effective at reducing aHRR. This marginally higher pHRR is more than offset by the significantly higher effectiveness and durability of the LH3 and HH3 coatings. However, it may be difficult to accurately compare these coating in the cone as the chitosan–MMT coating was evaluated

on a 50% thinner substrate and on a polyester (used for filters) rather than polyether (used in furniture) based polyurethane foam.

The MMT loading on the substrate is the residual mass measured at 800 °C in air using thermogravimetric analysis (TGA) (see Fig. S1 in the ESI†). The mass% of the coating that is MMT is calculated using the TGA residual values and the coating mass values in Fig. 2. These values as a function of composition and the number of TLs are reported in Fig. 7.

The MMT mass% on the substrate trends with the coating mass on the substrate. Both the MMT content and coating mass (Fig. 2) are higher using the high polymer formulations (Fig. 7a) and with increasing numbers of TL. At 1 TL, the MMT content is similar for all the formulations ($0.9\% \pm 0.1\%$). At higher numbers of TL, the MMT mass% is 1.5 to 2.5 times higher in the high polymer formulations. Compared to the loading levels of other FRs (10% to 30% by mass), the MMT mass% in these coatings is comparatively low above 3 TLs (3% to 7% for high polymer and 1% to 3% for low polymer formulations). For a given polymer formulation (H or L), there is 0.5% to 1% by mass higher MMT loading using the higher MMT formulation.

The mass% MMT in the coatings followed a similar trend regardless of the formulation. At 1 TL, the coatings were highly

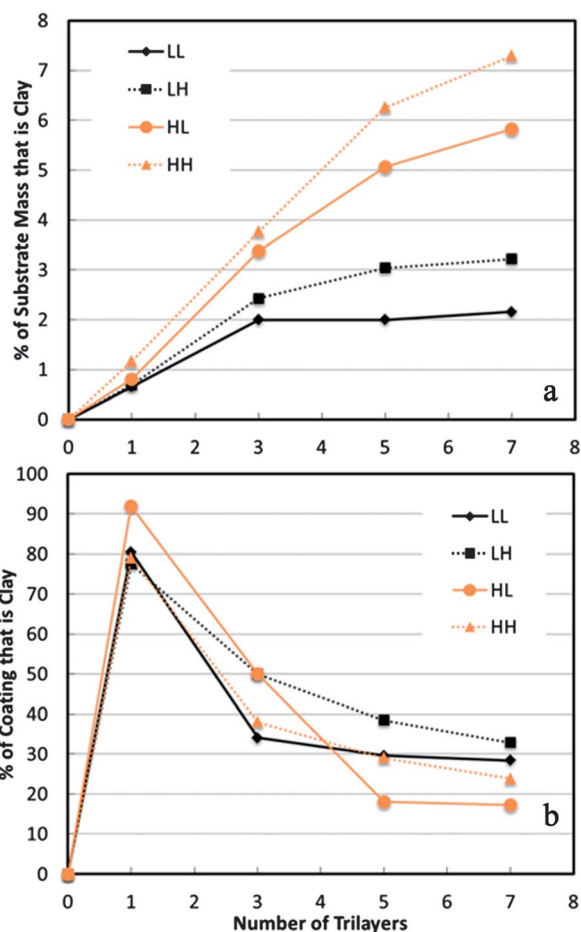


Fig. 7 MMT mass% on the substrate (a) and in the coating (b) as a function of the number of TLs deposited on the foam.

MMT (80% to 90% by mass). At 3 TLs, the coatings were more balanced in composition (35% to 50% by mass MMT). At higher numbers of TL, the MMT content slightly decreased further (20% to 35% by mass MMT). There is no strong trend based on formulation, except that the MMT content in the coating trends slightly higher in the low polymer formulations.

LH3 appears to be the best formulation as it provides the best flammability reduction with the least number of layers and lowest mass gain to the substrate. Combining the TGA and cone data also provides insight into characteristics that should be targeted for maximizing the fire retardant effect of the MMT LbL coatings and it may be an excellent starting point for the evaluation of other LbL FR technologies for PUF.

(1) Targeting a coating mass of 5% to 10%. For all formulations below a 5% coating mass (1 TL), the pHRR is reduced approximately 20% and there is still a significant second HRR peak. Above a 5% to 10% coating mass (5 TLs and 7 TLs) the flammability is significantly reduced. However, in the best FR formulations (HH ~ LH) there is no added FR benefit to having more than 3 TLs or 10% coating mass. More specifically, at or above 3 TLs for HH and LH there is no second peak, a similar reduction in aHRR ($76\% \pm 2\%$ HH and $72\% \pm 1\%$ LH) and similar reduction in pHRR ($27\% \pm 4\%$ for HH and LH). Therefore, for best performance, a 5% to 10% mass coating should provide a near maximum reduction in flammability that is achievable with that specific formulation.

(2) Using a high nanoparticle formulation. The most effective and durable FR coatings used a high MMT formulation, which may suggest using high concentration formulations for other nanoparticle FR (nanoFR). For a given MMT formulation, the impact on pHRR and aHRR was independent of polymer formulation. Therefore, choice of a polymer concentration should be based on other factors; *e.g.*, cost, final product mass, or filler content. For example, if a requirement is to minimize the product mass, the 3 TL LH should be used because the 3 TL HH produces a similar fire reduction, but is 1.5 to 2.5 times heavier.

(3) Targeting a nanoFR mass of 20% to 50% of the coating. At or above 3 TLs, the MMT accounts for 20% to 50% by mass of the coating for all the formulations. In general, more MMT is needed when the coating is more polymer-rich and heavier. This is extremely important as it helps the researcher decide whether to change formulations or just increase the number of layers. If within a few layers the MMT (or perhaps another nanoparticle) loading is relatively low (*e.g.*, 20% to 30% by mass), then consider switching to another formulation rather than increasing the number of layers. If the mass content is relatively high (*e.g.*, 40% to 50%), then continue depositing until the desired flammability reduction is achieved, which should be within a few more layers. These observations should be comparable when using other nanoFR.

Mechanical and physical properties of treated PU foam

PUF has a broad range of applications (*e.g.*, cushioning in furniture and transportation) where the comfort level, as defined by ASTM 3574 for residential applications, is adjusted

by changing the isocyanate, polyol, additives, and processing conditions. To use this LbL FR technology, it is essential to understand how these coatings impact the mechanical and physical properties that define specifications for commercial residential foam.

Two sale specifications for PUF residential applications are Indentation Force Deflection (IFD, firmness) and Support Factor (SF). 25% IFD is defined as the force required to displace a foam specimen by 25% of the thickness. Typical IFD₂₅ values range from (24 to 45) pounds per 50 inch². Higher IFD values indicate a firmer foam. SF, also known as the compression modulus, is defined as the ratio of 65% IFD to 25% IFD. SF typically ranges from 1.8 to 3 with a higher number indicating a more cushioning foam.⁴⁵ This test is traditionally performed on larger foam (50.0 cm by 50.0 cm by 10.2 cm (thickness)) than coated and tested in this study (10.2 cm by 10.2 cm 5.0 cm (thickness)). Therefore, the IFD and SF values presented here should be used only to understand the impact of the coatings relative to the others in this study and not used to compare with values reported elsewhere.

Examples of loading–displacement (LD) curves are provided in Fig. 8, and the testing values for all formulations are provided

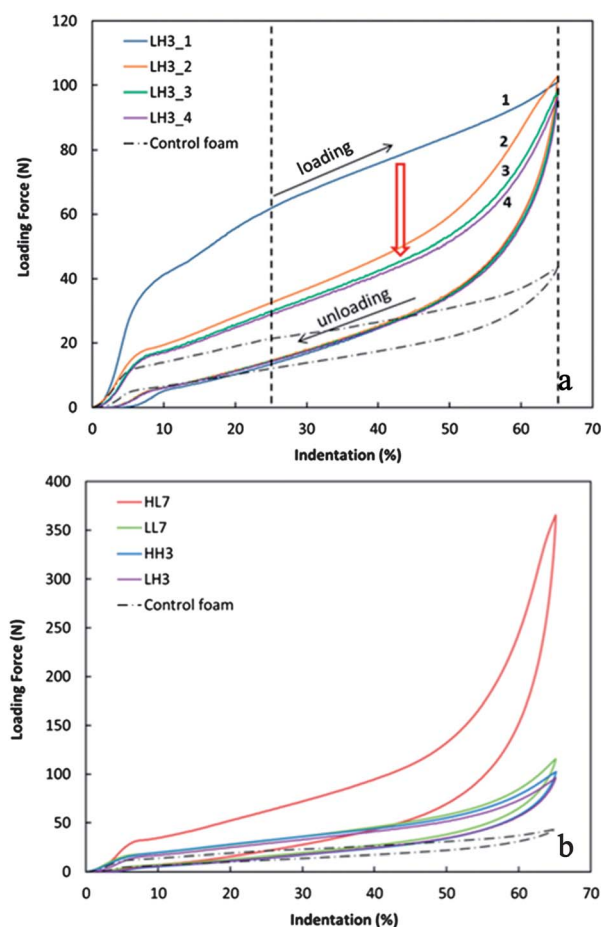


Fig. 8 Loading–displacement curves for (a) uncoated PUF (first compression cycle) and LH3 as a function of the number of compression cycles and (b) for the best flammability reduction with the least number of TLs for each formulation (fourth compression cycle).

Table 2 % IFD, support factor and % hysteresis of control foam and coated foams (after 4 compression cycles)

	Coating mass %	Applied 25% IFD (N)	Applied 65% IFD (N)	Recovery 25% IFD (N)	SF	% Hysteresis
Control	—	21.4	43.6	12.1	2	56.5
LL1	0.7	24.6	71.7	12.2	2.9	49.7
LL3	5.7	27.9	92.8	13.8	3.3	49.7
LL5	7.1	28.1	75.8	15	2.7	53.5
LL7	8	31.8	115.7	15.9	3.6	50.1
LH1	1	23.5	76.1	12.1	3.2	51.4
LH3	4.8	29	96.5	14.2	3.3	48.9
LH5	8.2	31.4	117.8	15.3	3.7	48.7
LH7	9	34.5	110.7	14.9	3.2	43.2
HL1	0.8	24.2	72.2	12.2	3	50.6
HL3	7.5	33.9	119.1	14.4	3.5	42.4
HL5	27.4	65.7	332.9	21.4	5.1	32.5
HL7	31.2	62.3	351.8	21.2	5.6	34.1
HH1	1.5	26.7	78.7	13.1	2.9	49
HH3	9.9	31.9	102.3	14.2	3.2	44.3
HH5	21.5	45.8	208	19.5	4.5	42.7
HH7	30.6	50.1	196.3	21.6	3.9	43.1

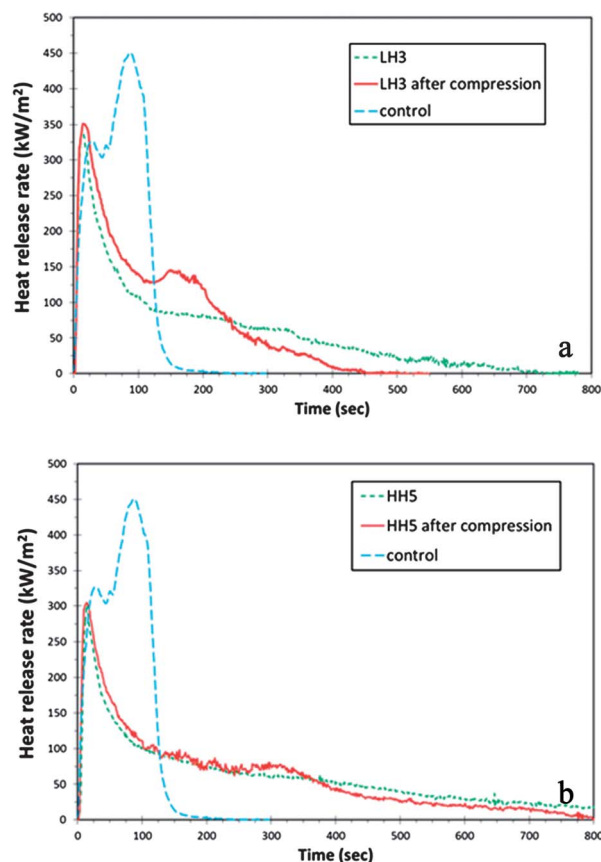
in Table 2. All of the formulations increased the stiffness of the PUF to a degree dependent on the mass and the polymer composition of the coating. However, even though the loading force values are higher after the initial compression, the LD curves characteristics are quite similar to the uncoated PUF. An example for one of the best flammability coatings (LH3) is provided in Fig. 8a. The applied curve has significantly decreased with the second cycle while the 65% IFD value and the recovery curve appear unchanged. The only measurable change with the third and fourth cycle is a slight decrease in the 65% IFD value. While the IFD values are still higher than the pure PUF, it appears that a few compression cycles are sufficient to significantly recover much of the lost flexibility. This same behavior was observed for the formulations. Since the PUF flexibility can quickly be recovered by a few compression cycles it was decided that a more useful comparison to the end-use application of LbL was to measure IFD and SF values on the coated PUF on the fourth compression cycle. Since the PUF values do not change after four cycles, the values provided are on the first cycle.

The values provided in Table 2 and the LD curves in Fig. 8b are for PUF (first cycle) and the coated PUF (fourth cycle). The 25% and 65% IFD values increase with increasing numbers of TL. Regardless of the formulation, the values are comparable for all the 1 TL and for all the 3 TL formulations. This is because the coating mass is similar for the 1 TL formulations and the 3 TL formulations. Compared to pure PUF, all 1 TL formulations have comparable 25% IFD values, but 1.8 times higher 65% IFD values. At 5 TLs to 7 TLs the high polymer formulations have a 3 and 4 times, respectively, higher coating mass and hence these formulations (HH and HL) have significantly higher 25% and 65% IFD. Once the displacement head is retracted to 25%, the force needed to maintain a 25% compression (recovery 25% IFD) was very similar to pure PUF for all the 1 TL and 3 TL formulations. The low polymer 5 TL and 7 TL formulations

(LL and LH) had slightly higher recovery 25% values, whereas the high polymer formulations had 1.5 times higher values. % Hysteresis return, which is the percentage of the return 25% IFD divided by the applied 25% IFD, is used to quantify perceived comfort.⁴⁶ The higher the value the greater the perceived comfort. Similar % hysteresis return values suggest that the coated PUF may be as comfortable as the untreated PUF.

LD curves for the best flammability reduction with the least number of TLs are provided for each formulation; *i.e.*, LL7, HL7, LH3, and HH3 (Fig. 8b). Except for HL7, the LD curves are very similar for these formulations. HH3 and LH3 provided the greatest reduction in flammability and have very similar LD curves, IFD and SF values; therefore, either of the formulations would appear to be a viable option for further evaluation for commercialization. Though the LH3 and HH3 values are still slightly higher than pure PUF, these values may still be within acceptable ranges and/or another PUF product could be coated where the coatings enable it to be within typical product specifications.

To understand whether the flexibility recovered came at the sacrifice of the FR integrity of the coating, the LH3 and HH5 substrates were tested in the cone calorimeter (Fig. 9) after the fourth compression cycle. For HH5 this led to a 10% increase in the aHRR, but for LH3 there was a 77% increase in the aHRR as a second peak reappeared. However, the flammability reduction

**Fig. 9** Heat release rate of LH3 (a) and HH5 (b) foam after the compression and aging.

of the LH3 is still better than any other LbL FR coating previously reported on PUF.

Another critical performance specification for PUF is air permeability. Compared to PUF, there was no statistical difference in the permeability regardless of the formulation or the number of TLs. This is because the few hundred nanometer thick coatings on the cell walls are insignificant compared to the 100 micron to 200 micron diameter pores. Therefore, there is no need to evaluate this attribute in further LbL studies.

Conclusions

The impact of the LbL coatings on PUF is strongly dependent on the polymer and MMT concentration in the depositing solutions. Higher polymer concentrations (BPEI and PAA) resulted in rapid coating growth with as high as a 33% increase in the PUF mass with seven TLs. Due to this increased mass these coatings tended to make the PUF stiffer, but after compressing a few times most of the flexibility was regained without sacrificing flammability. Higher MMT concentrations slowed down the coating growth (as high as a 9% increase in the PUF mass at seven TLs); however, it was critical to flammability reduction. Using less than half the number of TLs, the high MMT formulations yielded a similar reduction in pHRR (about 30%) and nearly doubled the reduction in aHRR (about 75%). Compared to pure PUF, one of the best formulations (LH3) resulted in a 30% reduction in pHRR and a 80% reduction in aHRR with only a 4.8% increase in the substrate mass with only three TLs. This is the most significant aHRR reduction reported using a LbL coating indicating that this is the most effective and durable LbL FR coating reported to date on PUF. After several compressions of the coated PUF, the flammability reduction was only slightly compromised, but this technology still outperformed all previously reported LbL FR coatings. The coatings were only a few hundred nanometers thick so they had no impact on the PUF air permeability. Though the load-displacement curves indicate that the coatings can slightly stiffen PUF, the faster recovery without any permanent loss of flexibility suggests that these coatings will not negatively influence the comfort of the PUF when used in furniture or mattresses.

Acknowledgements

The authors thank Mr Szabolcs Matko for assisting in the airflow measurement, and Mr Anthony Giuseppetti from the Paffenbarger Research Center of American Dental Association Foundation for the compression testing of the foam.

Notes and references

- G. Decher, in *Multilayer Thin Films: Sequential Assembly of Nanocomposite Materials*, ed. G. Decher and J. B. Schlenoff, Wiley-VCH, Weinheim, Germany, 2003.
- P. T. Hammond, *AIChE J.*, 2011, **57**, 2928–2940.
- P. Schaaf, J.-C. Voegel, L. Jierry and F. Boulmedais, *Adv. Mater.*, 2012, **24**, 1001–1016.
- W. B. Stockton and M. F. Rubner, *Macromolecules*, 1997, **30**, 2717–2725.
- H. Lee, R. Mensire, R. E. Cohen and M. F. Rubner, *Macromolecules*, 2011, **45**, 347–355.
- J. Q. Sun, T. Wu, F. Liu, Z. Q. Wang, X. Zhang and J. C. Shen, *Langmuir*, 2000, **16**, 4620–4624.
- B. Mu, C. Lu and P. Liu, *Colloids Surf., B*, 2011, **82**, 385–390.
- M. Altman, A. D. Shukla, T. Zubkov, G. Evmenenko, P. Dutta and M. E. van der Boom, *J. Am. Chem. Soc.*, 2006, **128**, 7374–7382.
- A. Van der Heyden, M. Wilczewski, P. Labbe and R. Auzely, *Chem. Commun.*, 2006, 3220–3222.
- K. Ariga, J. P. Hill and Q. Ji, *Phys. Chem. Chem. Phys.*, 2007, **9**, 2319–2340.
- H. Lee, Y. Lee, A. R. Statz, J. Rho, T. G. Park and P. B. Messersmith, *Adv. Mater.*, 2008, **20**, 1619–1623.
- S. Y. Wong, L. Han, K. Timachova, J. Veselinovic, M. N. Hyder, C. Ortiz, A. M. Klibanov and P. T. Hammond, *Biomacromolecules*, 2012, **13**, 719–726.
- Y. Zhao, Y. W. Tang, X. G. Wang and T. Lin, *Appl. Surf. Sci.*, 2010, **256**, 6736–6742.
- K. Sheng, H. Bai, Y. Sun, C. Li and G. Shi, *Polymer*, 2011, **52**, 5567–5572.
- C. A. da Silva, M. Vidotti, P. A. Fiorito, S. I. Córdoba de Torresi, R. M. Torresi and W. A. Alves, *Langmuir*, 2012, **28**, 3332–3337.
- K. Ariga, Q. Ji, M. J. McShane, Y. M. Lvov, A. Vinu and J. P. Hill, *Chem. Mater.*, 2011, **24**, 728–737.
- M. Delcea, H. Möhwald and A. G. Skirtach, *Adv. Drug Delivery Rev.*, 2011, **63**, 730–747.
- Z. Y. Tang, Y. Wang, P. Podsiadlo and N. A. Kotov, *Adv. Mater.*, 2006, **18**, 3203–3224.
- V. Gribova, R. Auzely-Velty and C. Picart, *Chem. Mater.*, 2011, **24**, 854–869.
- S. Takahashi, K. Sato and J. I. Anzai, *Anal. Bioanal. Chem.*, 2012, **402**, 1749–1758.
- R. M. Iost and F. N. Crespilho, *Biosens. Bioelectron.*, 2012, **31**, 1–10.
- M. Michel, V. Toniazzi, D. Ruch and V. Ball, *ISRN Mater. Sci.*, 2012, **2012**, 13.
- Y.-C. Li, J. Schulz, S. Mannen, C. Delhom, B. Condon, S. Chang, M. Zammarano and J. C. Grunlan, *ACS Nano*, 2010, **4**, 3325–3337.
- Y.-C. Li, S. Mannen, A. B. Morgan, S. Chang, Y.-H. Yang, B. Condon and J. C. Grunlan, *Adv. Mater.*, 2011, **23**, 3926–3931.
- Y.-C. Li, S. Mannen, J. Schulz and J. C. Grunlan, *J. Mater. Chem.*, 2011, **21**, 3060–3069.
- F. Carosio, G. Laufer, J. Alongi, G. Camino and J. C. Grunlan, *Polym. Degrad. Stab.*, 2011, **96**, 745–750.
- F. Carosio, J. Alongi and G. Malucelli, *J. Mater. Chem.*, 2011, **21**, 10370–10376.
- A. Laachachi, V. Ball, K. Apaydin, V. Toniazzi and D. Ruch, *Langmuir*, 2011, **27**, 13879–13887.
- Y. S. Kim, R. Davis, A. A. Cain and J. C. Grunlan, *Polymer*, 2011, **52**, 2847–2855.
- G. Laufer, C. Kirkland, A. A. Cain and J. C. Grunlan, *ACS Appl. Mater. Interfaces*, 2012, **4**, 1643–1649.

- 31 Y. S. Kim, R. Harris and R. Davis, *ACS Macro Lett.*, 2012, **1**, 820–824.
- 32 M. Zammarano, R. H. Kramer, R. Harris, T. J. Ohlemiller, J. R. Shields, S. S. Rahatekar, S. Lacerda and J. W. Gilman, *Polym. Adv. Technol.*, 2008, **19**, 588–595.
- 33 S. Nazare and R. Davis, *Fire Sci. Rev.*, 2012, **1**, 1.
- 34 R. D. Davis, Y. S. Kim, R. H. Harris, M. R. Nyden, N. M. Uddin and T. Thomas, in *Interagency Agreement Final Report: Exposure and Fire Hazard Assessment of Nanoparticles in Fire Safe Consumer Products*, The National Institute of Standards and Technology, 2011.
- 35 Certain commercial equipment, instruments or materials are identified in the paper in order to specify the experimental procedure adequately. Such an identification is not intended to imply recommendations or endorsement by the National Institute of Standards and Technology, nor is it intended to imply that the materials or equipment identified are necessarily the best available for this purpose.
- 36 The policy of NIST is to use metric units of measurements in all its publications, and to provide statements of uncertainty for all original measurements. In this document, however, data from organizations outside NIST are shown, which may include measurements in non-metric units or measurements without uncertainty statements.
- 37 M. Zammarano, R. H. Kramer, S. Matko, M. Smith, S. Mehta, J. W. Gilman and R. D. Davis, in *NIST Technical Note 1747: Factors Influencing the Smoldering Performance of Polyurethane Foam*, National Institute of Standards and Technology, June 2012.
- 38 Y. H. Yang, M. Haile, Y. T. Park, F. A. Malek and J. C. Grunlan, *Macromolecules*, 2011, **44**, 1450–1459.
- 39 P. Podsiadlo, M. Michel, J. Lee, E. Verploegen, N. W. S. Kam, V. Ball, J. Lee, Y. Qi, A. J. Hart, P. T. Hammond and N. A. Kotov, *Nano Lett.*, 2008, **8**, 1762–1770.
- 40 Y. M. Lee, D. K. Park, W. S. Choe, S. M. Cho, G. Y. Han, J. Park and P. J. Yoo, *J. Nanosci. Nanotechnol.*, 2009, **9**, 7467–7472.
- 41 M. A. Priolo, D. Gamboa and J. C. Grunlan, *ACS Appl. Mater. Interfaces*, 2010, **2**, 312–320.
- 42 Y. H. Yang, F. A. Malek and J. C. Grunlan, *Ind. Eng. Chem. Res.*, 2010, **49**, 8501–8509.
- 43 F. A. Cotton and G. Wilkinson, in *Advanced Inorganic Chemistry: A comprehensive Text*, Wiley, New York, 1980.
- 44 N. H. Tran, G. R. Dennis, A. S. Milev, G. S. K. Kannangara, M. A. Wilson and R. N. Lamb, *J. Colloid Interface Sci.*, 2005, **290**, 392–396.
- 45 Information is from PFA Polyurethane Foam Association, <http://www.pfa.org>.
- 46 H. W. Wolfe, in *Mechanics of Cellular Plastics*, ed. H. W. Hilyard, Macmillan, New York, 1979, pp. 99–142.